MANUFACTURING METALLIC PARTS WITH DESIGNED MESOSTRUCTURE VIA THREE-DIMENSIONAL PRINTING OF METAL OXIDE POWDER

Christopher B. Williams, David W. Rosen
The George W. Woodruff School of Mechanical Engineering
Georgia Institute of Technology
813 Ferst Drive, Atlanta, GA, 30332-0405
(404) 894-9668, david.rosen@me.gatech.edu

Reviewed, accepted September 5, 2007

ABSTRACT

Cellular materials, metallic bodies with gaseous voids, are a promising class of materials that offer high strength accompanied by a relatively low mass. In this paper, the authors investigate the use of Three-Dimensional Printing (3DP) to manufacture metallic cellular materials by selectively printing binder into a bed of metal oxide ceramic powder. The resulting green part undergoes a thermal chemical post-process in order to convert it to metal. As a result of their investigation, the authors are able to create cellular materials made of maraging steel that feature wall sizes as small as 400 μm and angled trusses and channels that are 1 mm in diameter.

Keywords: Additive Manufacturing, Three-Dimensional Printing, Cellular Materials, Designed Mesostructure

1. ADDITIVE MANUFACTURING OF PARTS WITH DESIGNED MESOSTRUCTURE

1.1 Parts with Designed Mesostructure

Through the interspersion of gaseous voids into a metallic body, manmade cellular materials offer high strength accompanied by a low-density. Cellular materials can also offer high stiffness, high impact-absorption, and thermal and acoustic insulation [1]. Recent research has focused in designing the mesoscopic topology (the geometric arrangement of solid phases and voids within a material or product on the size range of 0.1 to 10 mm) of cellular materials for multiple design objectives. Examples include Wang and coauthors' acetabular cup (Figure 1a), in which the porosity of the truss structure has been designed to match the porosity of the recipient's bone so as to encourage bone growth upon implantation [2], and a trussed robot arm (Figure 1b) that has been optimized to minimize mass while meeting strength and deflection constraints [3].

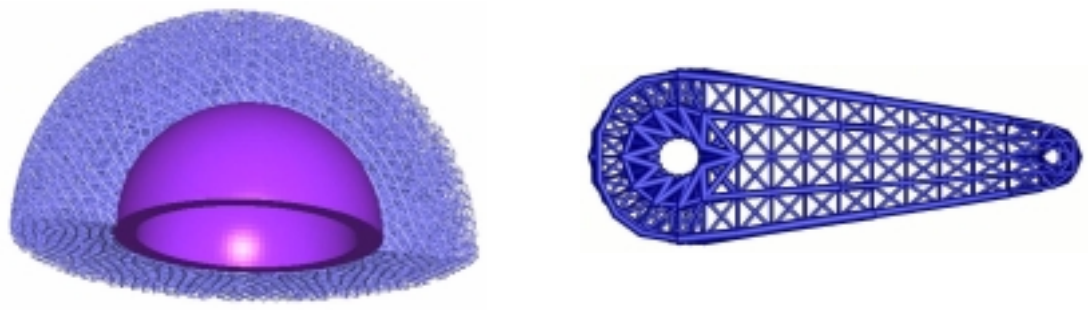

(a) (b)

Figure 1. Parts of designed mesostructure: (a) acetabular cup [2], (b) trussed robot arm [3]

Unfortunately, parts with designed mesostructure, like those shown in Figure 1, cannot be realized with traditional cellular material manufacturing processes. Due to the limitations imposed by these manufacturing processes, cellular materials are limited to either a random assortment of voids (e.g., metal foaming processes such as Hydro, Alporas, Formgrip, etc.) or an ordered repetition of a unit cell (e.g., honeycomb creation via sheet metal crimping and stamping). While such processes are capable of

producing light-weight and strong cellular materials, the imposed constraints on part macrostructure, material selection, and cellular mesostructure topology prevent a designer from creating the ideal cellular material for specific design intent(s) [4].

1.2 Metallic Cellular Materials via Additive Manufacturing

Because of the layer-based building process, additive manufacturing (AM) technologies offer the utmost geometric freedom in the design and manufacture of an artifact. As such, there are several research efforts that address the limitations of traditional cellular materials manufacturing via the use of direct-metal AM technologies to create parts of designed mesostructure. In general, direct-metal AM approaches are not ideal for manufacturing cellular materials due to limitations from poor resolution, poor surface finish, poor material properties, limited material selection, and need for support structures [4].

Ultrasonic consolidation, a technology which uses solid-state joining techniques to deposit two-dimensional swatches of metal tape, has been used to create closed honeycombs with walls with an aspect ratio of 100:1. However, because the sonotrode must have a sufficient area on which to operate, free-standing, unsupported, and/or angled ribs and trusses cannot be built with this process [7].

Selective Laser Melting (SLM) [5], Electron Beam Melting (EBM) [6], and Direct-Metal Laser Sintering have been successfully used to create parts with trussed or cellular material. These technologies offer a sufficiently small feature size for the creation of cellular materials, and they offer a fully-dense part directly out of the powder bed. These AM technologies which raster a one-dimensional energy source (e.g., laser or electron beam spot) over a powder bed of metal have inherent limitations, however. The use of high-powered energy source can introduce residual stresses, defects on bottom-facing surfaces, and can curl and/or warp the part during the build. As such, support structures, which can be difficult to remove from small cells, must be added to the part geometry. In addition, the entire powder bed must be pre-sintered before a layer is deposited; this pre-sintered powder can be difficult to remove from the cells of the finished part. Finally, these processes are generally expensive (due to a dependence on a high-powered energy source) and have slow build rates (due to a dependence on rastering a one-dimensional patterning spot).

1.3 Context

In an effort to address the limitations of existing cellular material manufacturing techniques, the authors have developed a new process for the realization of metal parts with designed mesostructure. Specifically the authors have augmented the three-dimensional printing process (3DP) for the creation of green parts (formed from metal oxide ceramic powders) that are suitable for conversion to metal via thermal chemical post-processing.

In this paper, the authors characterize process parameters that are pertinent to the creation of parts with designed mesostructure such as minimum wall thickness and minimum pore size. In Section 2, the two fundamental components of the process, three-dimensional printing and reduction of metal oxide powders, are presented. The manufacturing process is detailed in Section 3. Results are presented in Section 4 and closure is offered in Section 5.

2. THREE-DIMENSIONAL PRINTING OF METAL OXIDE POWDERS

The manufacturing process chain proposed by the authors is presented in Figure 2. The first step involves spray-drying fine metal oxide powders with a binder to form granules suitable for recoating with the 3DP machine. The second step features the formation of the ceramic green part via 3DP. The final step is a thermal chemical post-processing procedure that converts the metal oxide ceramic green part to metal. In this section, each phase of the process is detailed and a rationale for its inclusion is presented.

2.1 Chemically Converting Metal Oxide Green Parts to Metal via Reduction

Recognizing the limitations and difficulties present in directly additively manufacturing metals (as described in Section 1.2), the authors look to the creation of metal parts through the thermal chemical reduction of metal oxide precursors. This idea was inspired by the work of Georgia Tech's Lightweight Structures group with creating metallic linear cellular alloys (Figure 3) [8].

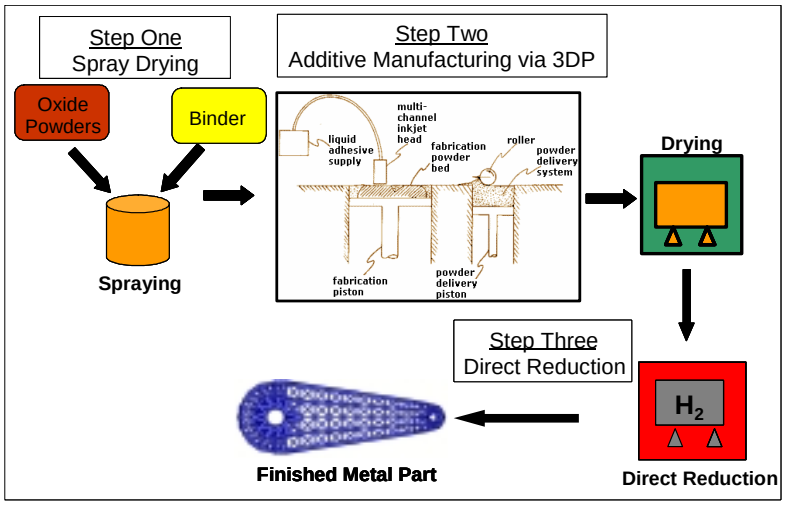

Figure 2. Manufacturing Process Chain of 3DP of Metal Oxide Powders and Reduction Post-Process

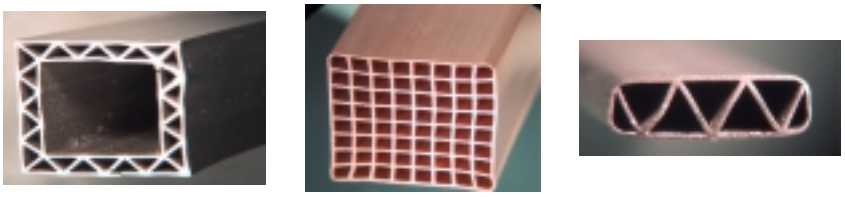

Figure 3. Linear Cellular Alloys

The linear cellular alloy manufacturing process features the extrusion of a metal oxide-based ceramic paste (containing lubricants, binders, and other additives) through an interchangeable die at room temperature. The ceramic green body is then dried, and processed in a reducing atmosphere to chemically convert the precursor into a metallic artifact [9]. The reducing agent is typically a gas (e.g., hydrogen or carbon monoxide), which reacts with the oxygen and forms water vapor, which is then removed from the system.

A wide variety of materials can be processed with this reduction technique. The primary requirement for a metal oxide is that it must be reducible at moderate temperatures (below the melting points of the materials involved) with a partial pressure of oxygen no lower than 10^{-16} atm. Unfortunately some elements such as Ti and Al are stable under these conditions; hence, they cannot be introduced into the alloy as an oxide, and must be added in a secondary process. With this technique, Cochran and coauthors have successfully processed a number of transition metal oxides (Fe, Ni, Co, Cr, Cu, Mo, W, Mn, and Nb), as well as many engineering alloys including stainless steel, maraging steel, Inconel, and Super Invar [10]. Through metallurgical characterization Cochran and coauthors have demonstrated that "the direct reduction metal is comparable to conventionally processed counterparts" [8]. Copper parts have demonstrated high thermal conductivity, and high strength and energy absorption have been demonstrated for maraging steel cellular structures.

Cell sizes in the range of 0.5 to 2.0 mm with web thicknesses of 50 to 300 μm have been fabricated with this process [8]. These small features are accomplished, in part, by the shrinkage (and large increase in density) that is accompanied with the reduction process. Shrinkage is typically on the order of 30 to 70% by volume; this can be advantageous when fine geometric features are desired that otherwise would be difficult or expensive to fabricate [10]. It is important to note that this large amount of shrinkage can cause cracks, laminations, disruption of dimensional stability, and/or warping if not controlled carefully [9].

Chemical reduction of metal oxide green parts to metal has the potential to alleviate many of the limitations found in direct-metal AM of cellular materials. An implementation of this post-processing technique is economically efficient, as the cost differential between a metal oxide powder and its metal counterpart is usually better than a 1-to-10 ratio [10]. Fine oxide powders are readily available in a pure and stable form. Compared to pure metal powders, metal oxides are safer as they are neither carcinogenic nor explosive.

It is also important to note that while a wide-range of geometries can be theoretically made using this process, the structure must be open for the article to survive the conversion process and emerge as a monolithic product. In general, the requirement for the geometry is to have a high surface-to-volume ratio and a highly open access to the interior. Multiple openings provide an unrestricted passage of both the reducing agents (hydrogen) to and the reaction products (water) from the interior [9]. It is also important that the structure does not have a widely varied thickness throughout its cross-section; an equal coercion force in the structure is needed so that it will survive the large shrinkage that takes place in the reduction process [10].

2.2 Three-Dimensional Printing of Spray-Dried Powder

Having decided to combine additive manufacturing with reduction post-processing, the authors were faced with the following design task: to design a layer-based AM process that is capable of creating green cellular parts composed of metal oxide ceramic material that are suitable for thermal chemical post-processing. Following a systematic conceptual design and preliminary selection process (as described in [11]), the authors identified three-dimensional printing (3DP) as an appropriate AM technology for the realization of parts with designed mesostructure [12].

3DP features the selective printing of a binder over a bed of powder via an array of inkjet nozzles [13]. The parallel deposition of the multiple nozzles enables the 3DP technology to deposit entire portions of a layer in a single pass, thus dramatically increasing its build speed. The two-dimensional patterning process implemented by 3DP can also be scaled cost effectively since it does not require an expensive laser element [14]. Furthermore, the use of an inkjet printing nozzle to pattern binder provides the 3DP technology the ability to create parts with high resolution (minimum feature size of ~0.1 mm), which is a crucial requirement for the realization of cellular materials. The use of inkjet printing technology also enables the creation of the cross-sections that are characteristic of cellular materials. This is not true of all AM patterning techniques; extrusion processes, for example, are unable to satisfactorily deposit the small, discrete ellipses typically found in truss structure cross-sections (Figure 4) due to pores created by poor optimization of material flow, filament/roller slippage, liquefier head motion, and build/fill strategies [15].

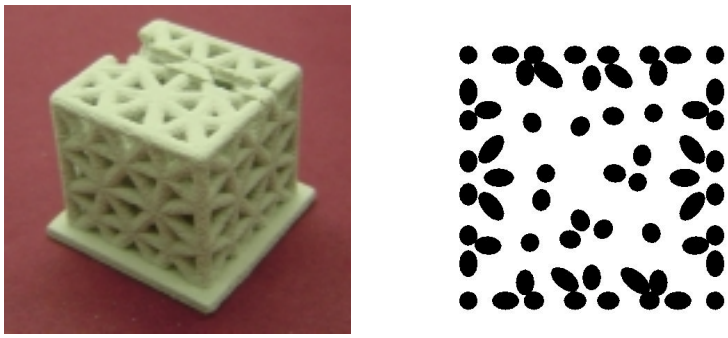

Figure 4. Patterning Truss Structure: (a) trussed cube, (b) characteristic cross-section

Another advantage of using 3DP is its use of a powder bed. Many AM technologies must create support structures to facilitate the construction of over-hanging features. Such structures are not desirable when creating parts with designed mesostructure because they would be near-impossible to remove from the parts' small pores and channels. By building a part in a powder bed, the need for support structures is eliminated as the un-patterned powder can support the complex geometry. One drawback of the powder bed, however, is that un-patterned powder can be trapped in, or, at the very least, troublesome to remove from the complex cellular geometries.

In general, the primary concern with ceramic AM technologies is in creating a green part with a sufficient solids loading percentage for it to be suitable for sintering and reduction (i.e., to easily reach full density and to minimize warping, curling, and shrinkage). By working with the powder in its raw, loose form, 3DP avoids the solids loading and rheology constraints found in the other ceramic AM technologies that work with powder/binder suspensions (e.g., aqueous [16] and hot-melt [17] direct inkjet printing, extrusion [18], and stereolithography [19]). Due to the use of a powder bed, the maximum solids loading of a green part created via 3DP is limited only by the tap density of the powder (which itself is dependent on particle size, shape, and distribution). Utela and coauthors have observed powder beds with as high as

55 vol% in their work with 3DP [20]. Compared to other ceramic AM processes (35 vol% solids in direct hot-melt inkjet printing [17], 40 vol% solids in extrusion [21]), 3DP has a relatively high green part solids loading.

Research involving the 3DP of ceramics encountered early setbacks because of the use of single-phase ceramic powders. The fine powders needed for high powder bed density and good sintering characteristics do not flow well enough during the recoating process to spread into defect-free layers [13]. In an effort to work with fine powders and to increase green part density, Grau and coauthors augmented the 3DP process to print onto a substrate formed by a dried powder/binder slurry [22]. Kernan and coauthors have used slurry-based 3D Printing of a tungsten carbide mixture with post-processing in a reducing atmosphere to create tungsten carbide-cobalt [23]. While the green part density increased to 67%, build time dramatically increased and the unpatterned material became extremely difficult to remove, a problem for the delicate features found in cellular materials [24].

In order to circumvent the recoating problems associated with working with fine particles, the authors choose to spray-dry the working powder. Spray-dried powders are spherical, homogeneous, 20 μm sized granules that are composed of smaller micron-sized powder particles held together by a small amount of binder [25]. As such, the granules are of a suitable size for the recoating process, while still allowing the use of fine particles for their sintering benefits. While the porous nature of spray-dried powders is detrimental in that it slightly decreases the solids loading possible for a green part, it is beneficial since smaller primitives result from the increased absorption of the jetted binder [26].

3. EXPERIMENTAL PROCEDURE

3.1 Material Preparation

While a wide variety of transition metal oxides can be reduced to metal using the procedure described in Section 2.1, we have chosen to work with maraging steel in this work. Maraging steel features high strength and high fracture toughness. Through small changes in the composition of its constituents, it is possible for the material to have a variety of mechanical properties; thus one can imagine easily altering the mixture ratios in order to achieve specific design objectives. Maraging steel also has uniform, predictable shrinkage during heat treatment. Finally, its constituents are easily reduced (Table 1). A metal oxide powder system that will chemically convert to maraging steel upon reduction was created by combining iron oxide (Fe_3O_4), nickel oxide (NiO), cobalt oxide (Co_3O_4), and molybdenum metal (Mo) powders and ball milling them for 24 hours.

Table 1. Reduction Reactions of Maraging Steel Constituents

$Fe_3O_4 + 4H_2 \longrightarrow 3Fe + 4H_20$	(1)
$Co_3O_4 + 4H_2 \longrightarrow 3Co + 4H_20$	(2)
$NiO + H_2 \longrightarrow Ni + H_20$	(3)
Maraging Steel: Fe 18.5Ni 8.5Co 5Mo	

Once mixed, the metal oxide powder system was spray-dried with a poly-vinyl alcohol (PVA) binder. Two batches of spray-dried powder were prepared: one batch with 2 wt% PVA and one with 4 wt% PVA. PVA was chosen because it is a common binder that works well with almost any oxide ceramic [27]. The resulting granules had a mean diameter of 25 μm.

3.2 Manufacturing Process Chain

Once spray-dried, the metal oxide granules are processed using a ZCorp Z402 three-dimensional printer. Sample parts are created by depositing ZCorp's ZB7 binder into the powder bed at a layer thickness of 100 μm. Once formed, the parts are left in the powder bed for 15 minutes to allow the binder to fully dry and for the green parts to gain strength. The green parts are then transferred to a depowdering station where unbound pattern is carefully removed from the complex cellular geometry using compressed air and a vacuum nozzle.

Once depowdered, the green parts are reduced and sintered in an atmosphere-controlled tube furnace in an Ar-10% H_2 environment using the cycle presented in Figure 5. Debinding of the PVA binder occurs at 450 C, reduction of the metal oxide green part occurs at 850 C, and sintering of the metal occurs at 1300 C.

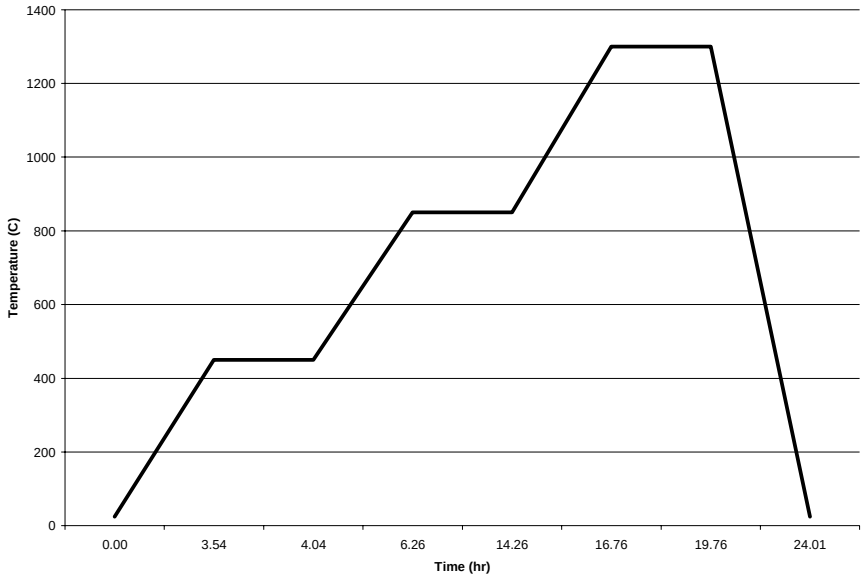

Figure 5. Cycle for Reduction and Sintering of Maraging Steel

4. RESULTS

4.1 Green Part Formation

Despite minimal process re-configuration, the green parts created via the deposition of ZB7 binder into the powder bed of spray-dried metal oxide granules were satisfactory. Aware that the spray-dried granules are more porous than standard ZCorp plaster powders, the saturation level (the amount of binder deposited over successive layers) was slightly increased from its default value. Other than this, no changes were made to the default printing setup.

Ballistic ejection of powder was observed in the deposition of the initial layers. As described in [28], this is caused from the significant kinetic energy that is associated with the impact of binder droplets. The resultant green parts had poor surface finish on their bottom-facing surfaces. This can be solved through adding a small amount of moisture via a mist to the powder bed in order to fixate the initial layers. This hypothesis is corroborated by the observation that no powder ejection occurred once the powder bed was wetted by the printing of the parts' first few layers.

Aside from the errors in the build direction caused by particle ejection, the green parts created by the process displayed very good dimensional accuracy. No shrinkage was observed in the creation of the green parts, thus no adjustments to the printer's anisotropic scaling settings were needed.

As is typical of all materials created by the 3DP process, the green parts were fragile coming out of the powder bed. While the presence of unbound powder is sufficient to support the parts during their removal from the bed, it is the depowdering of the green parts where one must be extremely cautious. As anticipated, the removal of unbound powder from small, closed channels proved to be the limiting factor in the type of geometry that could be created. Furthermore, while small walls and trusses could be printed, it was rare that they would survive the depowdering process.

4.2 Reduction and Sintering

Following the thermal treatment cycle shown in Figure 5, all sample parts were reduced and sintered to metal. Due to a low solids loading of the green part and the removal of the relatively large oxygen atoms through reduction, all parts created underwent a 46-50% linear shrinkage. Despite this large shrinkage,

none of the parts created displayed external evidence of warping or cracking (any flaws seen in the sample pictures below are attributed to green part cleaning).

The parts made from spray-dried powder with 2wt% PVA binder had an average relative density of 65.3%, while those made from the 4wt% PVA binder had an average relative density of 59.2% (as determined by the Archimedes method; theoretical density for maraging steel of 8.2 g/cc). The decrease in density of the parts prepared with the granules featuring 4wt% PVA binder is to be expected; the greater particle distance caused by the additional binder content inhibits densification during sintering. This is further corroborated by comparing the open porosity of the two samples: the granules with 2wt% PVA binder had an average open porosity of 29.8%, while those made with the 4wt% binder had an average open porosity of 36.4%. These results are summarized in Table 2.

Table 2. Density and Porosity Measurements After Reduction and Sintering

PVA weight %	Relative Density	Open Porosity
2 wt %	65.3%	29.8%
4 wt %	59.2%	36.4%

4.3 Cellular Material Characteristics

In an effort to characterize the proposed manufacturing process's ability to create parts of designed mesostructure, several test pieces with geometries typical of this special class of material were created. The sample parts are presented in both their green and sintered forms in Figures 6 – 9. Due to the size limitations of the tube furnace used to reduce and sinter the parts, the green parts are no larger than 10 mm in their cross-section.

The sample part shown in Figure 6 was created in order to discover the minimum wall thickness that is capable of being produced with the proposed manufacturing process. High-aspect ratio walls are prevalent in cellular materials as they provide channels for fluid flow in heat transfer applications as well as load bearing supports for structural applications. After sintering and reduction, the minimum wall thickness successfully built with this process is 400 μm.

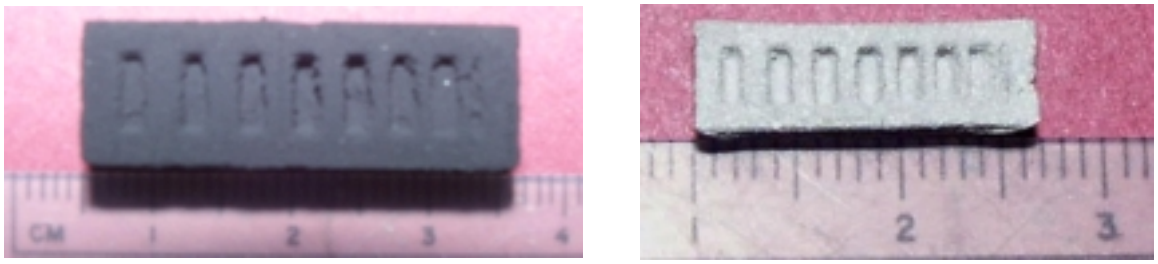

(a) (b)

Figure 6. Thin wall test: (a) green part, (b) sintered and reduced part

The sample parts shown in Figure 7 and 8 were created in order to test the ability of the process to realize parts with small channels and pores. While it was evident that the 3DP process has the resolution to create geometry with small voids, these parts were used to test the ability of the green parts to withstand the rigorous depowdering that was necessary to remove the unbound powder. The trussed cube shown in Figure 7a features open channels that are 2 mm square and 10 mm in length (with intersecting channel openings).

The part shown in Figure 8 features a channel of 5 mm square and 30 mm in length. Four trusses (2 mm in diameter in green state) span the channel. The unbound powder was easily removed from both of these sample parts via compressed air. Although these two test geometries were successfully created, it should be noted that there exists a limit to the size of channel that can be created with this process due primarily to an inability to remove unbound powder from small and/or closed channels. Through additional tests it was found that channels smaller than 2 mm in diameter (green state) could not consistently be depowdered; variation of success was dependent upon channel length and whether or not the channel was open on both ends.

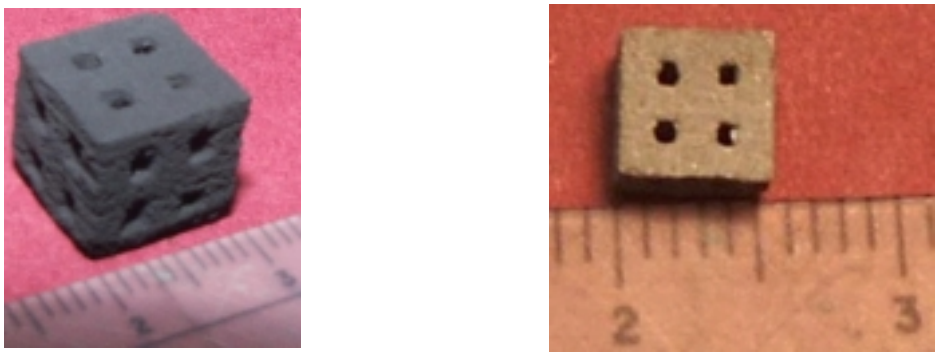

(a) (b)

Figure 7. Channel cube test: (a) green part, (b) sintered and reduced part

Figure 8. Sintered and reduced trussed channel test sample

The trussed channel shown in Figure 9 is identical to that shown in Figure 8, except it only has three walls. Two of the trusses in the channel (2 mm in diameter in green state; 0.92 mm in sintered and reduced state) are angled at 45 degrees across the gap.

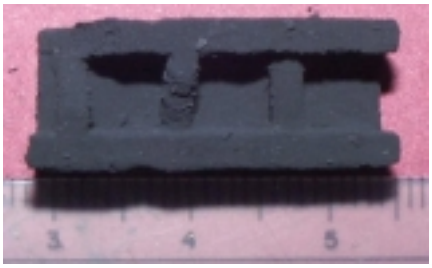

(a)

(b) (c)

Figure 9. Angled truss test: (a) green part, (b) & (c) sintered and reduced part

Thin, angled trusses are difficult to create in AM, as there is very little overlap between the bound material on each successive layer. Using Equation 4, the amount of overlap, x, can be calculated as a function of truss diameter, t, layer thickness, LT, and the angle of the truss, θ [6].

$$x = \frac{t}{\sin\theta} - \frac{LT}{\tan\theta} \tag{4}$$

With the successful manufacture of the trusses shown in Figure 9, we know that the process can successfully create trusses with layer overlaps of ≥ 2 mm. Additional tests are needed to identify the lower limit of this cellular material characteristic.

5. CLOSURE

In this paper the authors present a layer-based additive manufacturing process for the realization of metal parts with designed mesostructure. The process features the three-dimensional printing of spray-dried metal oxide ceramic powders followed by a post-production process wherein the green part is sintered and reduced in a hydrogen/argon atmosphere, thus chemically converting the part to metal. The process has been shown to successfully create parts with designed mesostructure. It is capable of creating walls as thin as 400 μm and channels as small as 0.92 mm in diameter. Angled trusses that are 1 mm in diameter have also been successfully fabricated.

When compared to the existing direct-metal AM technologies that are capable of producing cellular materials (e.g., Selective Laser Melting, Electron Beam Melting, and Direct Metal Laser Sintering), the process detailed in this paper is much less expensive. This cost savings is due to the working material (metal oxide powders can be up to 10 times cheaper than their metal counterparts) and to the technology itself (3DP machines cost roughly $500,000 less than a EBM machine due to the absence of an expensive, high-powered energy source such as a laser or electron gun, [29]). The two-dimensional material patterning found in 3DP also makes it much faster than those processes listed above which are limited by the need to raster a one-dimensional energy source.

A current limitation of the process is the resultant low sintered part density. In order to address this, the authors are exploring the printing of a solvent into the powder bed so as to activate the binder present in the spray-dried granule in the hope that the resultant deformation will bring the metal oxide particles closer together and thus improving the part's sintering characteristics. Printing a suspension of solvent and metal oxide nanoparticles into the powder bed could also increase green part density and reduce shrinkage during post-processing (as shown in [30] and [20]). Further future work is centered on the analysis of the metal parts that result from this process. X-ray diffraction and tensile and bending tests will provide insight into the material composition and strength of the parts, relatively.

6. ACKNOWLEDGMENTS

We gratefully acknowledge the funding given by NSF DMI-0522382. Christopher Williams acknowledges the financial support provided by the Georgia Tech Technical Innovation: Generating Economic Results (TI:GER) program (NSF IGERT – 0221600). Very special thanks are offered to Dr. Joe Cochran in the Materials Science and Engineering Department of Georgia Tech for sharing his wealth of knowledge and insight into the reduction and sintering post-process. Michael Middelmas is acknowledged for his assistance with the reduction and sintering post-process. The authors would also like to thank Mr. Joe Pechin of Aero-Instant Spray Drying Services of Brunswick, Georgia for his generosity and his assistance in preparing the spray-dried metal oxide powder systems.

7. REFERENCES

1. Banhart, J., 2000, "Manufacturing Routes for Metallic Foams," *The Member Journal of the Minerals, Metals & Materials Society,* Vol. 52, No. 12, pp. 22-27.

2. Wang, H. V., S. R. Johnston and D. W. Rosen, 2006, "Design of a Graded Cellular Structure for an Acetabular Hip Replacement Component," *17th Solid Freeform Fabrication Symposium*, Austin, TX, pp. 111-123.
3. Wang, H. and D. W. Rosen, 2002, "Computer-Aided Design Methods for Additive Fabrication of Truss Structures," *International Conference on Manufacturing Automation*, Hong Kong.
4. Williams, C. B., F. M. Mistree and D. W. Rosen, 2005, "Investigation of Solid Freeform Fabrication Processes for the Manufacture of Parts with Designed Mesostructure," *ASME IDETC Design for Manufacturing and the Life Cycle Conference*, Long Beach, California, DETC2005/DFMLC-84832.
5. Brooks, W., C. Sutcliffe, W. Cantwell, P. Fox, J. Todd and R. Mines, 2005, "Rapid Design and Manufacture of Ultralight Cellular Materials," *16th Solid Freeform Fabrication Symposium*, Austin, TX., pp. 231-241.
6. Cansizoglu, O., D. Cormier, O. Harrysson, H. West and T. Mahale, 2006, "An Evaluation of Non-Stochastic Lattice Structures Fabricateed Via Electron Beam Melting," *Solid Freeform Fabrication*, Austin, TX, pp. 209-2119.
7. Robinson, C. J., C. Zhang, G. D. Janaki Ram, E. J. Siggard, B. Stucker and L. Li, 2007, "Maximum Height to Width Ratio of Freestanding Structures Built Using Ultrasonic Consolidation," *Solid Freeform Fabrication Symposium*, Austin, TX., pp. 502-516.
8. Cochran, J. K., K. J. Lee, D. L. McDowell and T. H. Sanders, 2002, "Multifunctional Metallic Honeycombs by Thermal Chemical Processing," *Processing and Properties of Lightweight Cellular Metals and Structures (TMS)*, pp. 127-136.
9. Cochran, J. K., K. J. Lee and T. H. Sanders, 2003, "Metallic Articles Formed by Reduction of Nonmetallic Articles and Method of Producing Metallic Articles," US 6,582,651 B1, USA, Georgia Tech Research Corporation.
10. Cochran, J. K., K. J. Lee, D. McDowell, T. H. Sanders, B. Church, J. Clark, B. Dempsey, K. Hurysz, T. McCoy, J. Nadler, R. Oh, W. Seay and B. Shapiro, 2000, "Low Density Monolithic Metal Honeycombs by Thermal Chemical Processing," *Fourth Conference on Aerospace Materials, Processes, and Environmental Technology*, Huntsville, AL.
11. Williams, C. B., F. M. Mistree and D. W. Rosen, 2005, "Towards the Design of a Layer-Based Additive Manufacturing Process for the Realization of Metal Parts of Designed Mesostructure," *16th Solid Freeform Fabrication Symposium*, Austin, TX, pp. 217-230.
12. Williams, C. B. and D. W. Rosen, 2007, "Manufacturing Cellular Materials via Three-Dimensional Printing of Spray-Dried Metal Oxide Ceramic Powder," *3rd International Conference on Advanced Research in Virtual and Rapid Prototyping*, Leiria, Portugal.
13. Yoo, J., M. J. Cima, S. Khanuja and E. M. Sachs, 1993, "Structural Ceramic Components by 3D Printing," *Solid Freeform Fabrication Symposium*, Austin, TX., pp. 40-50.
14. Carrion, A., 1997, "Technology Forecast on Ink-Jet Head Technology Applications in Rapid Prototyping," *Rapid Prototyping Journal,* Vol. 3, No. 3, pp. 99-115.
15. Agarwala, M. K., V. R. Jamalabad, N. A. Langrana, A. Safari, P. J. Whalen and S. C. Danforth, 1996, "Structural Quality of Parts Processed by Fused Deposition," *Rapid Prototyping Journal,* Vol. 2, No. 4, pp. 4-19.
16. Wright, M. J. and J. R. G. Evans, 1999, "Ceramic Deposition Using an Electromagnetic Jet Printer Station," *Journal of Materials Science Letters,* 18, pp. 99-101.
17. Seerden, K. A. M., N. Reis, J. R. G. Evans, P. S. Grant, J. W. Halloran and B. Derby, 2001, "Ink-Jet Printing of Wax-Based Alumina Suspensions," *Journal of the American Ceramic Society,* Vol. 84, No. 11, pp. 2514-2520.
18. Lewis, J. A., 2000, "Colloidal Processing of Ceramics," *Journal of the American Ceramic Society,* Vol. 83, No. 10, pp. 2341-2359.
19. Griffith, M. L. and J. W. Halloran, 1996, "Freeform Fabrication of Ceramics via Stereolithography," *Journal of the American Ceramic Society,* Vol. 79, No. 10, pp. 2601-2608.
20. Utela, B., R. L. Anderson and H. Kuhn, 2006, "Advanced Ceramic Materials and Three-Dimensional Printing (3DP)," *17th Solid Freeform Fabrication Symposium*, Austin, TX, pp. 290-303, pp. 290-303.
21. Grida, I. and J. R. G. Evans, 2003, "Extrusion Freeforming of Ceramics through Fine Nozzles," *Journal of European Ceramic Society,* Vol. 23, pp. 629-635.

22. Grau, J., J. Moon, S. Uhland, M. J. Cima and E. Sachs, 1997, "High Green Density Ceramic Components Fabricated by the Slurry-Based 3DP Process," *Solid Freeform Fabrication Symposium*, Austin, TX., pp. 371-378.
23. Kernan, B. D., E. M. Sachs, M. A. Oliveira and M. J. Cima, 2003, "Three Dimensional Printing of Tungsten Carbide-Cobalt Using a Cobalt Oxide Precursor," *Solid Freeform Fabrication Symposium*, Austin, TX., pp. 616-631.
24. Moon, J., J. Grau and M. J. Cima, 2000, "Slurry Chemistry Control to Produce Easily Redispersible Ceramic Powder Compacts," *Journal of the American Ceramic Society,* Vol. 83, No. 10, pp. 2401-2408.
25. Reed, J. S., 1995, *Principles of Ceramics Processing*, John Wiley & Sons, Inc., New York.
26. Cima, M. J., A. Lauder, S. Khanuja and E. Sachs, 1992, "Microstructural Elements of Components Derived from 3D Printing," *Solid Freeform Fabrication Symposium*, Austin, TX., pp. 220-227.
27. Morse, T., 1979, *Handbook of Organic Additives for Use in Ceramic Body Formulation*, Montana Energy and MHD Research and Development Institute, Butte, MT.
28. Sachs, E., M. J. Cima, J. Cornie, D. Brancazio, J. Bredt, A. Curodeau, T. Fan, S. Khanuja, A. Lauder, J. Lee and S. Michaels, 1993, "Three-Dimensional Printing: The Physics and Implications of Additive Manufacturing," *CIRP Annals,* Vol. 42, No. 1, pp. 257-260.
29. Wohlers, T., 2006, *Wohlers Report 2006: Rapid Prototyping, Tooling & Manufacturing State of the Industry Annual Worldwide Progress Report*, Wohlers Associates, Inc., Fort Collins, Colorado.
30. Crane, N. B., J. Wilkes, E. Sachs and S. M. Allen, 2006, "Improving Accuracy of Powder-Based SFF Processes by Metal Deposition from a Nanoparticle Dispersion," *Rapid Prototyping Journal,* Vol. 12, No. 5, pp. 266-274.